Transverse Vibration Analysis of a Translating Roller-Follower Cam Using Cycloidal Profile for RDFD Motion 以擺線為 RDFD 運動輪廓的從動件凸輪之側向振動分析

Jer-Rong Chang¹ Ming-Chih Huang² Biing-Hwang Jou³ Heng-Pin Hsu^{4*} 張哲榮 ¹ 黄銘智 ² 周炳煌 ³ 許恆斌 ^{4*}

- ^{1,4} Department of Mechanical Engineering, Air Force Institute of Technology
 - ^{2, 3} Department of Aircraft Engineering, Air Force Institute of Technology

1,4 空軍航空技術學院機械工程科 2,3 空軍航空技術學院飛機工程系

Abstract

The transverse vibration of a translating roller-follower cam due to the flexible follower rod is investigated. The theory of envelopes is applied to determine the cam profile. Cycloidal profile is used to design the rise-dwell-fall-dwell (RDFD) motion of the follower. The follower is modeled as a Rayleigh beam. The rigid-body translation is coupled with the flexible deformation and thus causes the study to become a moving boundary problem. Since the transverse deflection of the follower is considered, the contact position of the roller and the cam is an unknown which cannot be determined only with kinematics analysis. The unknown position will be substituted into the dynamics modeling with considering the geometric constraints. Applying the assumed mode method and Hamilton's principle, the governing equations of motion are derived to be non-linear differential-algebraic equations. The system vibration responses for the RDFD motion are obtained using Runge-Kutta method. Then, the influences of system parameters are investigated.

Keywords: cam, roller-follower, cycloidal profile, translating, transverse vibration, RDFD

摘要

本文研究撓性從動桿所造成的平移式滾子從動件凸輪的側向振動。以包絡線理論決定一凸輪輪廓,以擺線輪廓設計從動件做指定的上昇-停滯-下降-停滯運動,從動件模擬為雷利樑。剛體位移與撓性變形耦合,使本研究成為一變邊界問題。由於考慮從動件的側向撓度,滾子與凸輪的接觸點為一未知,無法僅由運動學分析決定。以幾何限制的方式,將此未知位置代入動力模擬。使用假設模態法與漢彌頓原理,導出統御運動方程式,此方程式為非線性的微分代數方程式。以阮奇-庫達法求解系統振動響應,並進行系統參數影響的研究。

關鍵字:凸輪,滾子從動件,擺線輪廓,平移式,側向振動,上昇-停滯-下降-停滯

1. INTRODUCTION

The design and the analysis of cam mechanisms have been introduced and discussed extensively [1-3]. A cam is a common mechanism element that drives a mating component known as a follower. The unique feature of a cam is that it can impart a very distinct motion to its follower. Since the motion of a cam can be prescribed, it is well suited for applications where distinct displacements and timing are paramount. Cams are found in almost all machines, e.g. machine tools, internal-combustion engines, computers, and instruments.

A considerable amount of work on the study of cams has been reported. The great majority of researchers paid attention to the design of cams using kinematics analysis [4-7]. Some researchers investigated the dynamics of cams. In the dynamic analysis of cam mechanisms, two different mathematical models are used. One is a discrete system which has finite degrees of freedom. The other is an elastic system which has infinite degrees of freedom. Mathematical model with infinite degrees of freedom is fitted to physical model. In the dynamic analysis of a cam mechanism, especially under a high rotation speed of a cam, this model can be used to solve the vibrations of a cam mechanism more exactly. However, only a few researchers took the infinite degrees of freedom into consideration.

Followers driven by high-speed, dwell-type, rotating disk cams can exhibit undesirable residual vibrations during dwell. Felszeghy [8] studied a cam with a translating roller follower. He idealized the follower structure as a single degree-of-freedom, spring-mass-dashpot, linear system. These residual vibrations were obtained with closed-form solutions to the steady-state vibrations obtained with a circular convolution integral. The steady-state vibrations, which can extend over the entire cam cycle, were periodic and continuous. Pasin [9] studied a valve control mechanism of internal combustion engines. The longitudinal vibrations of the moving rod were neglected, and the rod was loaded by a variable axial force. The equation of bending vibrations of this rod was obtained using the classical bending theory and d'Alembert's principle. Then the partial differential equation with variable coefficients was reduced to a system of ordinary differential equations of second order with periodic coefficients using Galerkin method. The stability of the rod and consequently of the cam mechanism was investigated according to

the parameters of speed and stroke. Fabien, Brian [10] presented a new approach to designing dwell-rise-dwell profiles for cam follower systems. The cam profiles are designed such that perturbations in the system parameters have a reduced influence on the dynamic response. This is accomplished by minimizing the parameter sensitivity of output mass motion. Followers driven by high-speed, dwell-type, rotating disk cams can exhibit undesirable residual vibrations during dwell. Yilmaz and Kocabas [11] studied the longitudinal vibrations of a follower which is the linear active component of a cam mechanism. The basic Bernoulli method was applied to solve the partial differential equation which was supplied by taking the viscous damping factor into consideration. Felszeghy [12] studied a cam with a translating roller follower. He idealized the follower structure single degree-of-freedom, as spring-mass-dashpot, linear system. These residual vibrations were obtained with closed-form solutions to the steady-state vibrations obtained with a circular convolution integral. The steady-state vibrations, which can extend over the entire cam cycle, were periodic and continuous. Wang and Jiang [13] studied the cam mechanism which was developed on the equivalent concept and the method of lumped masses in dynamic modeling of cam mechanisms. The method of using double lumped equivalent masses located in two ends of a component to substitute the mass of it in modeling was put out and proved to be true. The proposed improved the accuracy of the dynamic model of cam mechanisms.

In this paper, a disk cam with a translating follower is studied. The follower rod is taken to be flexible. The rod pinned with a roller which is restrained with a rigid rotating cam groove. Since the follower is flexible, the contact point of the roller and the cam is an unknown though it locates at the Two geometric constraints profile. established and added to the Hamilton's principle with Lagrange multipliers. The transverse deflection of the follower is expanded with the assumed mode method in which the mode is time-dependent since the follower is driven to lengthen or shorten when the cam is rotating. The vibration response of the follower obtained from is the derived differential-algebraic equation by applying the Runge-Kutta integration method.

2. DERIVATION OF GOVERING EQUATIONS

A disk cam with a translating roller follower is shown in Fig. 1. The cam is assumed to be rigid. The roller follower consists of a follower rod that has a separate part, the roller, which is pinned to the follower stem. The follower rod is considered to be flexible and described by using Rayleigh beam theory. Since the roller moves in groove, the roller maintains contact with the cam and rolls on the cam surface as the cam rotates. The rigid-body motions and the flexible vibrations are restrained by the contact constraints.

The kinetic energy and strain energy of the follower, the kinetic energy of the roller, and the work done by the constraint forces are formulated first. The follower deflections are expanded using the assumed mode method. Then, the governing equations of the flexible follower rod are derived by employing Hamilton's principle.

2.1 The cam profile for RDFD case

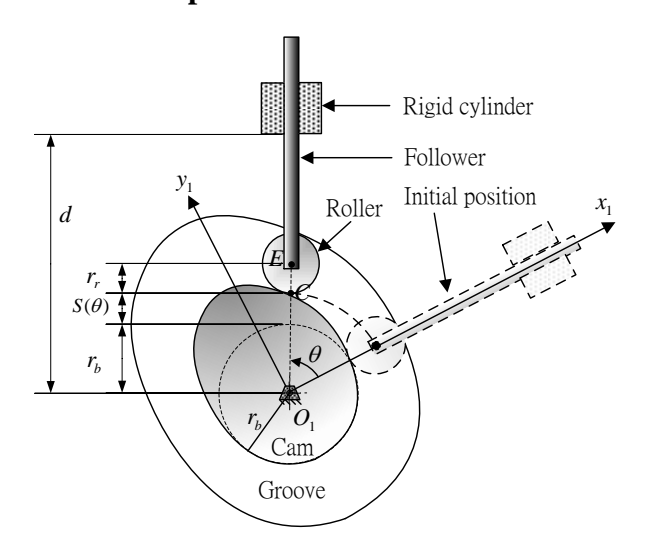


Fig. 1 Schematic of a translating roller-follower cam.

The schematic of a cam mechanism is shown in Fig. 1. The displacement function of the follower rod when the cam rotates an angle θ is denoted as $S(\theta)$. The rise-dwell-fall-dwell (RDFD) motion studied in this paper is described in Fig. 2. The cam profile is considered with rise and fall motions of cycloidal displacement (sinusoidal acceleration). The displacement function $S(\theta)$ for the rise segment is given with the following function: (Chen [2])

$$0 \le \theta \le \beta : S(\theta) = S_T \left[\frac{\theta}{\beta} - \frac{1}{2\pi} \sin(\frac{2\pi\theta}{\beta}) \right]$$
 (1)

where β is the period of the rise segment and S_T is the total lift magnitude. In this study, β is set to

be $\frac{\pi}{2}$. The above motion is used for the rise portion of the cam. The rise function is applicable to the fall with slight modification. To convert rise function to fall function, it is only necessary to subtract the rise displacement function $S(\theta)$ from the maximum lift S_T . The period of the fall segment is also set to be $\frac{\pi}{2}$.

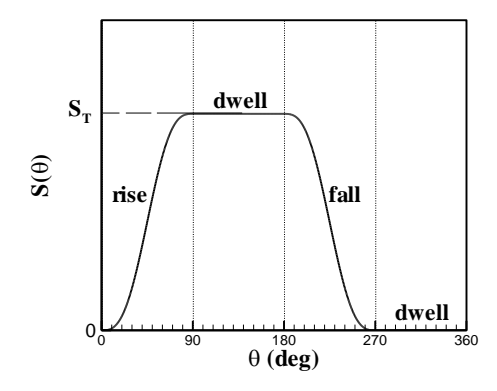


Fig. 2 The rise-dwell-fall-dwell (RDFD) motion.

Using the theory of envelopes, one can determine the cam profile. The profile coordinates (x_{1C}, y_{1C}) are derived as (refer to Fig. 1)

$$x_{1C} = r\cos\theta - \frac{r_r Q}{\sqrt{P^2 + Q^2}},$$

$$y_{1C} = r\sin\theta + (x - r\cos\theta)\frac{P}{Q}.$$
(2)

where

$$r = r_b + r_r + S(\theta),$$

$$P = r \sin \theta - S'(\theta) \cos \theta,$$

$$Q = r \cos \theta - S'(\theta) \sin \theta.$$
(3)

in which r_b is the base-circle radius of the cam, and r_r is the roller radius.

And the coordinates of the roller center E are

$$x_{1E} = r\cos\theta, y_{1F} = r\sin\theta.$$
 (4)

A rotating frame $O_1 - x_1y_1$ fixed on the cam which rotates with a constant angular speed Ω is

shown in Fig. 3. A fixed frame $O_2 - xy$ is also used and its unit coordinate vectors are denoted as $\{\mathbf{i}, \mathbf{j}\}^T$. The O_2x axis coincides with the centerline of the undeformed rod. The flexible follower undergoes a transverse deflection, v(x,t). The end point E moves to be E' after deformation. The transverse deflection at the end point E are denoted as v_E , i.e., $v_E = v(l,t)$. A fixed frame $O_1 - XY$ is also used. The fixed coordinates for the points C and E are

$$X_{C} = x_{1C} \sin \Omega t - y_{1C} \cos \Omega t,$$

$$Y_{C} = x_{1C} \cos \Omega t + y_{1C} \sin \Omega t,$$

$$X_{E} = x_{1E} \sin \Omega t - y_{1E} \cos \Omega t,$$

$$Y_{E} = x_{1E} \cos \Omega t + y_{1E} \sin \Omega t.$$
(5)

From the geometric relationship as shown in Fig. 3, two constraint equations for the point E are derived as

$$\Phi_1 = X_E - \nu_E = 0 \tag{6}$$

$$\Phi_2 = Y_E + x_E - d = 0 \tag{7}$$

It is seen that the rigid-body motion and the flexible vibration are coupled under the geometric constraints.

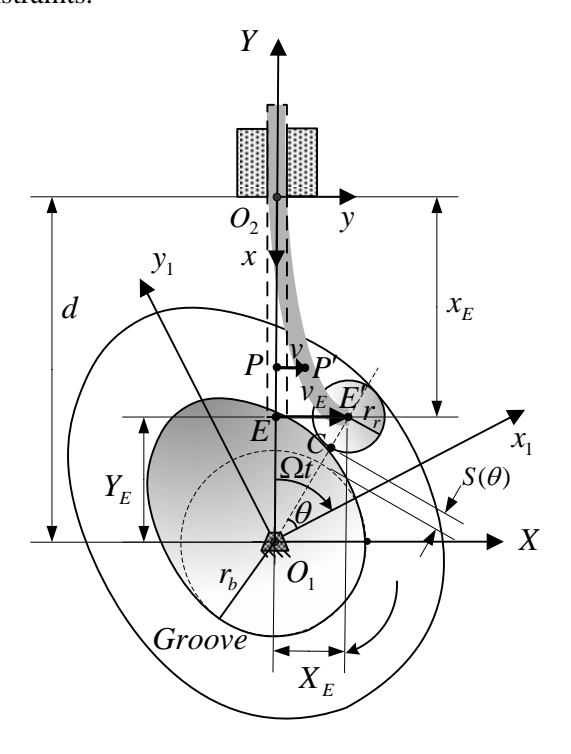


Fig. 3 Deformed configuration of the cam mechanism

2.2 The kinetic energy and strain energy of the system

2.2.1 The kinetic energy and strain energy of the rod

An arbitrary point P on a cross-section of the follower rod is deformed to be the point P', shown in Fig. 3. The position vector $\mathbf{R}_{P'}$ can be expressed as

$$\mathbf{R}_{P'} = (x - yv_x)\mathbf{i} + (y + v)\mathbf{j}$$
 (8)

where the subscript means to take partial derivative with respect to x.

The velocity of the point P' is derived as

$$\dot{\mathbf{R}}_{P'} = [\dot{x} - y\dot{v}_{x}]\mathbf{i} + \dot{v}\mathbf{j} \tag{9}$$

where the dot symbol means to take derivative with respect to time t.

The kinetic energy T_{rod} of the rod can be expressed as

$$T_{rod} = \frac{1}{2} \iiint_{V} \rho \dot{\mathbf{R}}_{P'} \cdot \dot{\mathbf{R}}_{P'} dV$$

$$= \frac{1}{2} \int_{0}^{x_{E}} \rho A(\dot{x}^{2} + \dot{v}^{2}) dx + \frac{1}{2} \int_{0}^{x_{E}} \rho I \dot{v}_{,x}^{2} dx$$
(10)

where ρ denotes the mass density of the rod. A is cross-sectional area of the rod. I is the area moment of inertia of the rod cross-section. It is known form Eq. (10) that the kinetic energy of the rod contains the rigid-body and flexible translational and rotational energies.

Applying the strain-stress relationship of Hooke's law, one has the strain energy U_{rod} of the rod as follows,

$$U_{rod} = \frac{1}{2} \iiint_{V} E(-yv_{,xx})^{2} dV = \frac{1}{2} \int_{0}^{x_{E}} EIv_{,xx}^{2} dx \quad (11)$$

where E denotes Young's modulus of beam material.

2.2.2 The kinetic energy of the roller

The kinetic energy of the roller including the

translational and rotational energies is derived as

$$T_{roller} = \frac{1}{2} m_r \dot{\mathbf{R}}_{E'} \cdot \dot{\mathbf{R}}_{E'} + \frac{1}{2} J_r \dot{\theta}_r^2$$

$$= \frac{1}{2} m_r (\dot{X}_E^2 + \dot{Y}_E^2)$$

$$+ \frac{1}{2} \frac{J_r}{r_*^2} [(\dot{X}_C - \dot{X}_E)^2 + (\dot{Y}_C - \dot{Y}_E)^2]$$
(12)

where m_r and J_r are the mass and the polar mass moment of inertia of the roller, respectively.

2.3 Assumed mode method

One end of the follower rod is restrained with a rigid cylinder and the other end is connected to the roller. For satisfying the boundary condition at the rigid cylinder end, one can expand the deflections by applying assumed mode method as follows,

$$v(x(t),t) = \sum_{i=2}^{N} b_i(t)x(t)^i$$
 (13)

where x^i is the mode shape which is dependent on time since the follower is driven by the cam to lengthen or shorten. $b_i(t)$ is the associated amplitudes for the transverse deflection. Though the polynomial expansion is a simple assumed mode method, it can easily formulate the moving boundary problem.

2.4 Hamilton's principle

Applying Hamilton's principle for the whole system, one has the variation equation

$$\int_{t_1}^{t_2} \delta(T_{rod} + T_{roller} - U_{rod} + \lambda_1 \Phi_1 + \lambda_2 \Phi_2) dt = 0 \quad (14)$$

where T_{rod} and T_{roller} are the kinetic energy of the follower rod and the roller, respectively. U_{rod} is the strain energy of the follower rod. $\lambda_1\Phi_1$ and $\lambda_2\Phi_2$ are the works done by the constraint forces.

Substituting equation (13) into Hamilton's principle (14), one can obtain the system equation of motion. The equation is expressed as

$$\mathbf{M}(\mathbf{Q})\ddot{\mathbf{Q}} + \mathbf{N}(\mathbf{Q}, \dot{\mathbf{Q}}) + \mathbf{\Phi}_{\mathbf{Q}}^{T} \lambda = \mathbf{0}$$
 (15)

where M, N, and λ are mass matrix, nonlinear

vector, and Lagrange multiplier, respectively. It is noted that the mass matrix is time-dependent. \mathbf{Q} is the generalized coordinates vector and expressed as

$$\mathbf{Q} = [b_1 \quad b_2 \quad \cdots \quad b_N \quad x_E \quad \theta]. \tag{16}$$

The two constraints as expressed in equations (6) and (7) are combined as the following form

$$\mathbf{\Phi}(\mathbf{Q}) = \begin{bmatrix} \Phi_1 & \Phi_2 \end{bmatrix}^T = \mathbf{0} \tag{17}$$

Differentiating equation (17) with respect to time, one has the constraint velocity equation

$$\mathbf{\Phi}_{\mathbf{Q}}\dot{\mathbf{Q}} + \frac{\partial \Phi}{\partial t} = \mathbf{0} \tag{18}$$

Then differentiating equation (18) with respect to time, one has the constraint acceleration equation

$$\mathbf{\Phi}_{\mathbf{Q}}\ddot{\mathbf{Q}} = -\left(\mathbf{\Phi}_{\mathbf{Q}}\dot{\mathbf{Q}}\right)_{\mathbf{Q}}\dot{\mathbf{Q}} - 2\frac{\partial\Phi_{\mathbf{Q}}}{\partial t}\dot{\mathbf{Q}} - \frac{\partial^{2}\Phi}{\partial t^{2}} \equiv \mathbf{\eta} \quad (19)$$

Combining the nonlinear ordinary differential equation (15) and the constraint acceleration equation (19), one obtains the following expression

$$\begin{bmatrix} \mathbf{M} & \mathbf{\Phi}_{\mathbf{Q}}^T \\ \mathbf{\Phi}_{\mathbf{Q}} & \mathbf{0} \end{bmatrix} \begin{bmatrix} \ddot{\mathbf{Q}} \\ \boldsymbol{\lambda} \end{bmatrix} = \begin{bmatrix} -\mathbf{N}(\mathbf{Q}, \dot{\mathbf{Q}}) \\ \boldsymbol{\eta} \end{bmatrix}$$
(20)

The above equation is the differential-algebraic equation which governs the vibration of the translating roller-follower cam mechanism.

3. SIMPLIFICATION OF DAE

Using the partitioning method [14], the generalized coordinate vector is partitioned as

$$\mathbf{Q} = \begin{bmatrix} \mathbf{p} & \mathbf{q} \end{bmatrix} \tag{21}$$

where

$$\mathbf{p} = [b_1 \quad b_2 \quad \cdots \quad b_N], \tag{22}$$

$$\mathbf{q} = [x_E \quad \theta] \tag{23}$$

Then, equation (20) can be rewritten as

$$\mathbf{M}^{pp}\ddot{\mathbf{p}} + \mathbf{M}^{pq}\ddot{\mathbf{q}} + \mathbf{\Phi}_{\mathbf{p}}^{T}\lambda = -\mathbf{N}^{p}$$

$$\mathbf{M}^{qp}\ddot{\mathbf{p}} + \mathbf{M}^{qq}\ddot{\mathbf{q}} + \mathbf{\Phi}_{\mathbf{q}}^{T}\lambda = -\mathbf{N}^{q}$$

$$\mathbf{\Phi}_{\mathbf{p}}\ddot{\mathbf{p}} + \mathbf{\Phi}_{\mathbf{q}}\ddot{\mathbf{q}} = \mathbf{\eta}$$
(24)

Eliminating λ and $\ddot{\mathbf{q}}$ from the above equation, one has the simplified second order nonlinear ordinary differential equation in independent generalized coordinate \mathbf{p} as

$$\hat{\mathbf{M}}(\mathbf{p})\ddot{\mathbf{p}} + \hat{\mathbf{N}}(\mathbf{p}, \dot{\mathbf{p}}) = 0 \tag{25}$$

where

$$\begin{split} \hat{\mathbf{M}} &= \mathbf{M}^{pp} - \mathbf{M}^{pq} \mathbf{\Phi}_{\mathbf{q}}^{-1} \mathbf{\Phi}_{\mathbf{p}} - \mathbf{\Phi}_{\mathbf{p}}^{T} \left(\mathbf{\Phi}_{\mathbf{q}}^{-1} \right) (\mathbf{M}^{qp} - \mathbf{M}^{qq} \mathbf{\Phi}_{\mathbf{q}}^{-1} \mathbf{\Phi}_{\mathbf{p}}), \\ \hat{\mathbf{N}} &= \left[\mathbf{N}^{p} - \mathbf{\Phi}_{\mathbf{p}}^{T} \left(\mathbf{\Phi}_{\mathbf{q}}^{-1} \right)^{T} (\mathbf{N}^{q} - \mathbf{F}^{q}) \right] \\ &+ \left[\mathbf{M}^{pq} \mathbf{\Phi}_{\mathbf{q}}^{-1} - \mathbf{\Phi}_{\mathbf{p}}^{T} \left(\mathbf{\Phi}_{\mathbf{q}}^{-1} \right)^{T} \mathbf{M}^{qq} \mathbf{\Phi}_{\mathbf{q}}^{-1} \right] \mathbf{\eta} \end{split}$$

Let $\mathbf{Z} = [\mathbf{p} \ \dot{\mathbf{p}}]$ be the state variable vector, one can rewrite (25) in terms of \mathbf{Z} as

$$\dot{\mathbf{Z}} = \begin{bmatrix} \dot{\mathbf{p}} \\ -\dot{\mathbf{M}}^{-1} \hat{\mathbf{N}} \end{bmatrix} \tag{27}$$

Applying the Runge-Kutta integration method to solve equation (27), one can obtain the vibration response of the follower.

4. NUMERICAL RESULTS AND DISCUSSIONS

An example is studied to investigate the vibration of the translating roller-follower cam for RDFD case. Since the follower is flexible, the contact point of the roller and the cam is an unknown point though it locates at the cam profile. The vibration response at the end point of the follower in the transverse direction is studied to show that the contact position between the cam and the roller of the flexible rod is different from that under the assumption of the rigid follower rod.

The cycloidal displacement motion is applied to model the rise and fall displacement curve. The period of the rise and fall segment β is set to be

 $\frac{\pi}{2}$. The total rise S_T is set to 15 mm. The cross section of the follower rod is a circle with radius of $r_f = 5$ mm. The associated cross-sectional area and $A = 78.54 \text{ mm}^2$ are inertia and area $I = 490.87 \text{ mm}^4$. The elastic modulus and the density of the follower rod $E = 2.1 \times 10^8 \text{ kg/mm} \cdot \text{s}^2$ and $\rho = 7.8 \times 10^{-6} \text{ kg/mm}^3$. The distance from the lower end of the rigid cylinder

and the rotation center of the cam is $d=112 \,\mathrm{mm}$. The base-circle radius of the cam is $r_b=26 \,\mathrm{mm}$. The radius, mass, and mass polar moment of inertia of the roller are $r_r=5 \,\mathrm{mm}$, and $m_r=0.05 \,\mathrm{kg}$, respectively.

The time step is set to be $\frac{2\pi}{\Omega} \times 10^{-3}$ s. The initial conditions are given as zero. To check the numerical convergence, three different mode numbers N=2,3,4 are applied to obtain the vibration responses for $\Omega=240 \text{ rad/s}$. Figure 4 shows the transverse vibration response at the end point E of the follower. It is seen that the responses curves with N=3 and N=4 almost coincide. This implies that the numerical results for the studied case nearly converge with N=3. In the following numerical study, the assumed mode method with N=3 is used.

The follower vibration with different rotation speed of cam is analyzed. The rotation speeds are $\Omega=120,\ 240,\ 360\ \text{rad/s}$, respectively. Figure 5 shows the transverse vibration response at the end point E. It is shown that the transverse response is more significant for higher cam rotation speed especially in the rise and fall intervals. The high frequency oscillation occurs. Even in the dwell interval the follower still oscillates. For high rotation speed of cam, the responses during the dwell interval are obviously larger than those for low rotation speed of cam. Thus, the deflections during the dwell interval for high rotation speed of cam are of significance to a certain extent.

The effect of the distance, d, from the lower end of the rigid cylinder and the rotation center of the cam on the vibration is studied. Three distances, 102, 112 and 122 mm are used. The vibraion results are shown in Fig. 6. The maximum response amplitudes are all higher for larger distance d. This may be explained that larger distance d combined with a longer follower rod makes lower stiffness of the rod to bring about larger response. It is also found that the distance influences the phase of the response. The follower cross-sectional radius effect is also studied. The vibration responses with three cross-sectional radii of the follower rod, 3, 5 and 7 mm, are compared in Fig. 7. It is seen that the vibration responses are larger for the smaller cross-sectional radius of the follower rod. This may

also be explained that smaller cross-sectional radius of follower rod makes lower stiffness of the rod.

The responses of the follower for three different cam base-circle radii are investigated. The results are shown in Fig. 8. It is found that the transverse response is larger for the smaller cam base-circle radius. Since the distance d remains the same for the three cam base-circle radii, the follower is relatively longer for the smaller cam base-circle radius and the vibration is more significant. Three different total rises are also studied. They are $S_T = 8$, 15 and 22 mm. It is seen from Fig. 9 that larger total rise induces larger vibration response.

5. CONCLUSIONS

The equations of motion for the vibration of a translating roller-follower cam for RDFD case are derived by using Hamilton's principle and the assumed mode method. The flexibility of the follower rod is considered and modeled as a Rayleigh beam. The roller motion is restrained in the cam groove under the follower deflections. Thus, two geometric constraints are formulated to be added to the Hamilton's principle with Lagrange multipliers. The numerical results for the studied cases show that the transverse vibration response of the follower is large for high rotation speed of cam. Even during the dwell interval, the follower vibrates to some extent especially for high rotation speed of cam. The follower rod with larger length or smaller cross-sectional radius induces larger response amplitude of the follower. The smaller cam base-circle radius or the larger total rise also brings about larger response amplitude.

REFERENCES

- Chakraborty, J., and Dhande, S. G., Kinematics and Geometry of Planar and Spatial Cam Mechanisms. John Wiley & Sons, 1977.
- 2. Chen, F. Y., Mechanics and Design of Cam Mechanisms, Pergamon Press, New York, 1982.
- 3. Koloc, Z., and Vaclavik, M., Cam Mechanisms, Elsevier, 1993
- 4. Bouzakis, K. D., Mitsi, S., and Tsiafis, J., Computer-aided optimum design and NC milling of planar cam mechanisms, Int. J. Mach. Tools Manufact., **37**(8), 1997, pp. 1131-1142.
- Yu, Q., and Lee, H. P., Optimum design of cam mechanisms with oscillating flat-face followers, Mechanics Research Communications, 23(2),

- 1996, pp. 181-187.
- 6. Lampinen, J., Cam shape optimization by genetic algorithm, Computer-Aided Design, **35**, 2003, pp. 727-737.
- 7. Biswas, A., Stevens, M., and Kinzel, G. L., A comparison of approximate methods for the analytical determination of profiles for disk cams with roller followers, Mechanism and Machine Theory, **39**, 2004, pp. 645-656.
- 8. Felszeghy, S. F., Steady-state residual vibrations in high-speed, dewll-type, rotating disk cam-follower systems, Transactions of the ASME, Journal of Vibration and Acoustics, **127**, 2005, pp. 12-17.
- 9. Pasin, F., On dynamic stability of followers in cam mechanisms, Mechanism and Machine Theory, **18**(2), 1983, pp. 151-155.
- 10. Fabien, Brian C., 1995, "The design of dwell-rise-dwell cams with reduced sensitivity to parameter variation," Journal of The Franklin Institute, Vol. 332, No. 2, pp. 195-209.
- 11. Yilmaz, Y., and Kocabas, H., The vibration of disc cam mechanism, Mechanism and Machine Theory, **30**(5), 1995, pp. 695-703.
- 12. Felszeghy, S. F., 2005, "Steady-state residual vibrations in high-speed, dewll-type, rotating disk cam-follower systems," Transactions of the ASME, Journal of Vibration and Acoustics, Vol. 127, pp. 12-17.
- 13. Wang, J., Jiang, Q., 2006, "A further study on the equivalent method of lumped masses in dynamic modeling of cam mechanisms," Journal of the Chinese Society of Mechanical Engineers, Vol. 27, No. 1, pp. 75-79.
- 14. Parviz, E. N., Computer-Aided Analysis of Mechanical System, Prentice-Hall International Edition, 1988, pp. 42-46.

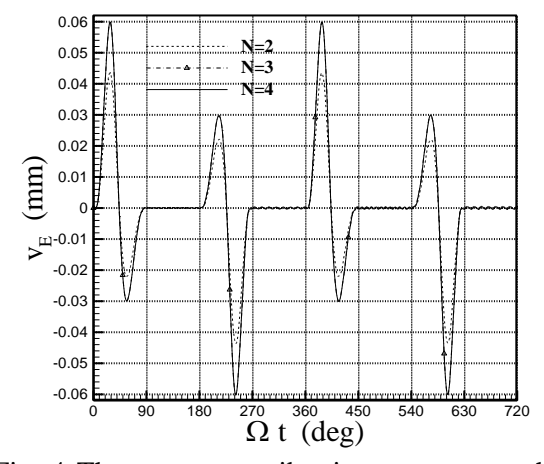


Fig. 4 The transverse vibration response at the end point E with different mode number for

航空技術學院學報 第十七卷 (民國一○七年)

 $\Omega = 240 \text{ rad/s}$.

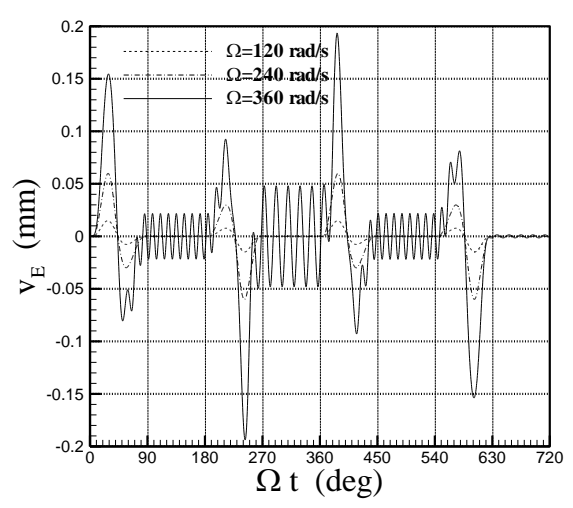


Fig. 5 The transverse vibration response at the end point E with different rotation speed Ω .

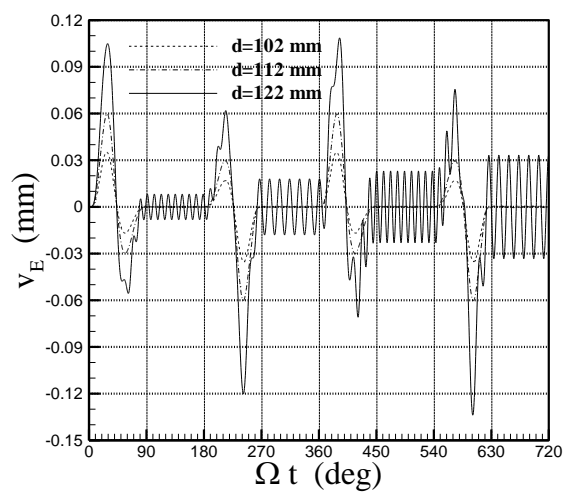


Fig. 6 The transverse vibration response at the end point E with different distance d.

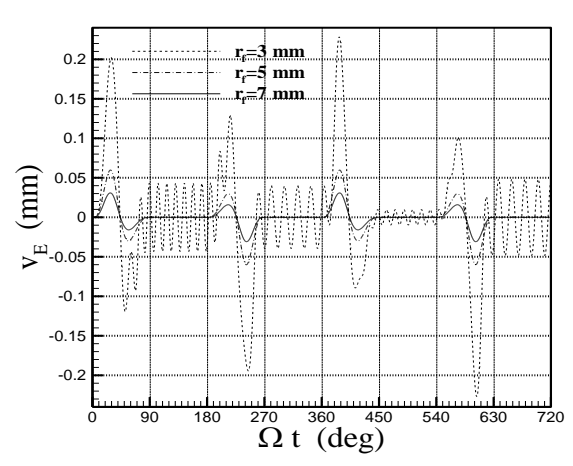


Fig. 7 The transverse vibration response at the end point E with different follower cross-sectional

radius r_f .

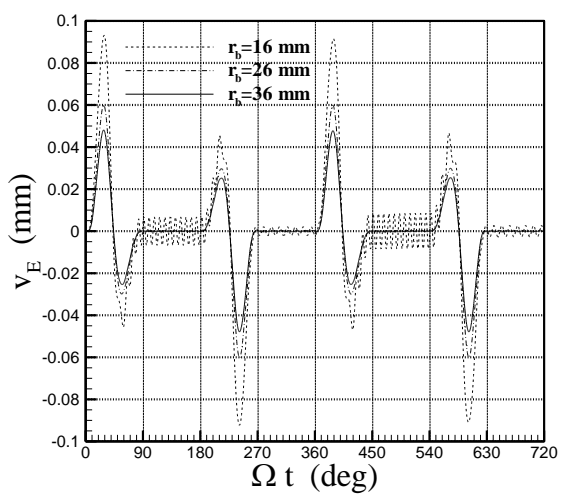


Fig. 8 The transverse vibration response at the end point E with different cam base-circle radius r_b .

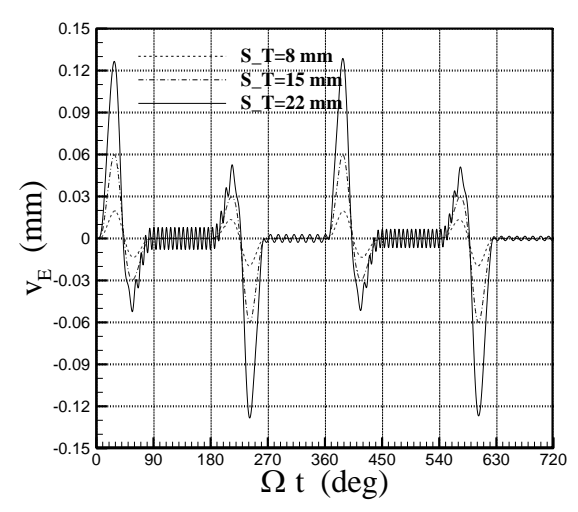


Fig. 9 The transverse vibration response at the end point E with different total rise S_T .